Zoosyst. Evol. 101 (4) 2025, 1513–1529 | DOI 10.3897/zse.101.156742

PENSOFT

für Natur MUSEUM FÜR NATURKUNDE BERLIN

An integrative analysis and account of two new species of *Dugesia* (Platyhelminthes, Tricladida, Dugesiidae) from the Hengduan Mountains, southwest China, with reflections on the historical biogeography of Eastern Palearctic/Oriental lineages

Fan Wu[1], Lei Wang[1], Ronald Sluys[2], Xin-Xin Sun[1], De-Zeng Liu[1], Zi-Mei Dong[1], Guang-Wen Chen[1]

1 *College of Life Science, Henan Normal University, Xinxiang, 453007, China*

2 *Naturalis Biodiversity Center, Darwinweg 2, 2333 CR Leiden, Netherlands*

https://zoobank.org/5B7A906E-8485-44B6-A20E-DBC0BAAF93FD

Corresponding authors: Zi-Mei Dong (dzmhjx@163.com); Guang-Wen Chen (chengw0183@sina.com)

Academic editor: Tom Artois ♦ **Received** 24 April 2025 ♦ **Accepted** 29 July 2025 ♦ **Published** 19 August 2025

Abstract

Two new species of the genus *Dugesia* from southwest China are described using an integrative approach based on morphological, histological, and molecular data. *Dugesia patula* Chen & Dong, **sp. nov.** is characterized by the following features: symmetrical openings of the oviducts into the bursal canal; vasa deferentia opening symmetrically into the mid-lateral portion of the seminal vesicle; a large and pointed diaphragm; a short duct between the seminal vesicle and diaphragm; and a very broad, short ejaculatory duct with a very wide opening at the tip of the penis papilla. *Dugesia postica* Chen & Dong, **sp. nov.**, is characterized by the following features: symmetrical openings of the oviducts into the bursal canal; a small penis bulb; a large and long penis papilla with a slightly larger dorsal lip and a small ventral lip; a long connecting duct between the seminal vesicle and diaphragm; a small diaphragm located near the tip of the penis papilla; and an extremely short ejaculatory duct. In the molecular phylogenetic tree, the two new species share a sister-group relationship and fall within an eastern Palearctic/Oriental clade of conspecifics. The distinct specific status of these two new species is also supported by their genetic distances. Through a multi-gene concatenated phylogenetic analysis, this study, for the first time, elucidates the evolutionary relationships among the Oriental, eastern Palearctic, and Australasian groups, enabling the development of a hypothesis on the potential dispersal routes of *Dugesia* into the eastern Palearctic region.

Key Words

COI, genetic distances, ITS-1, molecular phylogeny, taxonomy, 18S rDNA, 28S rDNA

Introduction

Approximately 115 species of the *Dugesia* Girard, 1850, have been reported from major parts of the Old World and Australia. Recently, taxonomic studies have begun to uncover the rich biodiversity present in China, revealing this region as a potential distribution hotspot for the genus (Solà et al. 2022; Wang et al. 2024). To date, fourteen species from China have been identified, with one species from northern China, three from central China, and ten from southern China (Wang et al. 2021; Chen et al. 2022; Wang et al. 2022; Wang et al. 2024).

The Hengduan Mountains, located in southwest China at the intersection of the Eurasian and Indian plates, are characterized by complex geological structures, varied climates, and a very rich biodiversity, hosting a large number of endemic species of both flora and fauna (Liu et al. 2022a, 2024; Cheng et al. 2024). Due to the collision of the Indian and Eurasian plates and the uplift of the Qinghai–Tibet Plateau, the Hengduan Mountains were formed,

while rivers were diverted. The glacial–interglacial cycles caused repeated shifts in the geographic location of suitable habitats, forcing organisms to disperse from the southwestern mountains to surrounding areas, thereby promoting species differentiation (Dong et al. 2020). During the Pleistocene, with its alternating glacial and interglacial periods, the high mountain valleys experienced severe habitat fragmentation, resulting in a significant so-called "sky island" isolation effect that accelerated species differentiation (Kandziora et al. 2022; Shi et al. 2023).

Although the presence of *Dugesia* in Kunming City, near the Hengduan Mountains, had already been reported by Liu (1989), species identification of the populations had not been carried out. However, previous research suggests that the species diversity of freshwater planarians within the Oriental Realm of China (including the Hengduan Mountains) may be severely underestimated (Solà et al. 2022; Wang et al. 2025, and references herein). In this paper, we add for the first time two new species of *Dugesia* to the fauna of southwest China by applying an integrative approach, using morphological, histological, and molecular data. In our analysis, we incorporated molecular sequences from many Asian species to improve resolution of their evolutionary relationships and determine the phylogenetic position of the two new species. In addition, this comprehensive phylogenetic study facilitated a more detailed analysis and resolution of the biogeographic patterns within the Asian group of *Dugesia* species, as compared with previous studies.

Materials and methods

Specimen collection and culturing

In 2019 and 2022, specimens were collected from various locations within Yunnan Province in southwest China (Fig. 1). The worms were transferred to plastic bottles filled with spring water and then placed in a cooler with ice packs for transport to the laboratory. These worms were cultured in autoclaved tap water at 16 °C and fed weekly with fresh beef liver. Prior to histological processing and DNA extraction, the worms were starved for at least one week. Images of their external morphology were captured using a digital camera attached to a stereo microscope.

Histology

The histological preparation processes were as previously described by Dong et al. (2017) and Wang et al. (2024). Worms designated for histological sectioning were first fixed in Bouin's solution for 24 hours, followed by rinsing and storage in 70% ethanol. Subsequently, the specimens were dehydrated through a graded series of ethanol solutions, cleared in clove oil, and embedded in paraffin. Ribbons of sections were prepared at intervals of 6 µm and stained with hematoxylin and Cason's Mallory–Heidenhain stain (Winsor and Sluys 2018). Photographs were taken with a Leica digital camera attached to a compound microscope. Histological preparations of the specimens will be deposited in the collections of the Zoological Museum of Henan Normal University, Xinxiang, China (ZMHNU), and Naturalis Biodiversity Center, Leiden, The Netherlands (RMNH).

DNA extraction, amplification, sequencing, and phylogenetic analysis

The procedures for DNA extraction, amplification, and sequencing followed those specified by Wang et al. (2025). Specific primers BarT and COIR were used to amplify fragments of the cytochrome c oxidase subunit I (COI) (Lázaro et al. 2009), while the internal transcribed spacer-1 (ITS-1), 18S ribosomal gene (18S rDNA), and 28S ribosomal gene (28S rDNA) were amplified using the primer pairs ITS9F and ITSR, 18S1F and 18S9R, and 28SMF1F, 28SMR1F, 28SMF2R, and 28SMR2R, respectively (Baguñà et al. 1999; Carranza et al. 1996; Stocchino et al. 2017). The polymerase chain reaction (PCR) was performed using Premix Ex Taq Hot Start Version (TaKaRa, Otsu, Japan). Purification and sequencing of PCR products were completed by GENEWIZ (Tianjin, China), using the same primers as those used for amplification. Both forward and reverse DNA strands of all specimens were sequenced. To ascertain the putative new species' taxonomic position within the genus *Dugesia*, phylogenetic analysis was conducted. A total of 70 samples (238 sequences), comprising 55 samples from known species and 15 from unidentified *Dugesia* specimens from Asia (Solà et al. 2022), were used for phylogenetic analysis and genetic distance calculations (GenBank accession numbers are provided in Table 1). These included the two new *Dugesia* species and three outgroup species, viz., *Schmidtea mediterranea* (Benazzi et al. 1975), *S. polychroa* (Schmidt 1861), and *Recurva postrema* Sluys & Solà, 2013.

Sequence alignment was conducted as previously described (cf. Katoh et al. 2019; Wang et al. 2024). Briefly, COI sequences were aligned using Translator X (http://translatorx.co.uk; Dessimoz and Gil 2010) with the FFT-NS-2 method of MAFFT and checked using BioEdit 7.2.6.1. Subsequently, sequences were back-translated into nucleotide sequences, totaling 705 base pairs (bp). ITS-1 sequences were aligned online with MAFFT (Online Version 7.247; https://mafft.cbrc.jp/alignment/server/) using the G-INS-i algorithm, totaling 761 bp. 18S rDNA and 28S rDNA sequences were aligned online with MAFFT v. 7.247 using the L-INS-i algorithm, totaling 1569 bp and 1386 bp, respectively. The four alignments were checked using MEGA v. 7 (Kumar et al. 2016) and concatenated in the following order using the "Concatenate Sequence" option in the PhyloSuite software: 18S rDNA–ITS-1–28S rDNA–COI (4317 bp). In the concatenated sequences, missing data were coded as "?".

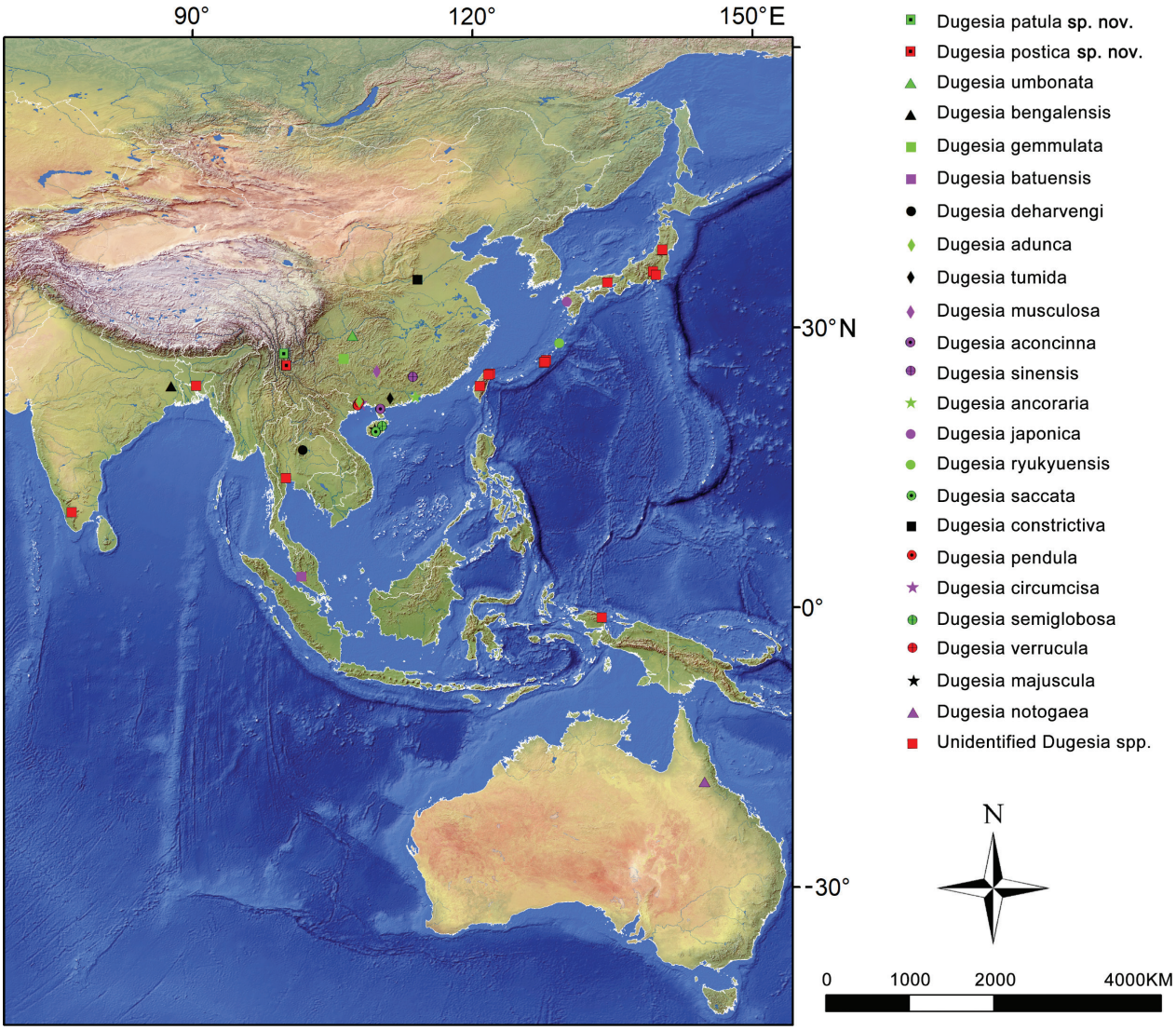

Figure 1. Map showing the distribution of *Dugesia* species across Asia and Australia, including the collection localities of the new species from Yunnan Province, China.

The best-fit evolutionary models for each gene and codon position were determined using PartitionFinder2 (Lanfear et al. 2017). The optimal evolutionary models selected for the concatenated dataset were as follows: GTR+G for ITS-1; GTR+I+G for 18S rDNA and 28S rDNA; GTR+I+G for the first and third codon positions of COI; and HKY+I+G for the second codon position of COI. Single-gene analyses yielded identical model selections for each respective gene and codon position. Phylogenetic trees were constructed using both maximum likelihood (ML) and Bayesian inference (BI) methods. ML analyses were conducted using IQ-TREE v1.6.2 with 10,000 standard bootstrap repetitions (Nguyen et al. 2015). BI analyses were performed in MrBayes v3.2 (Ronquist et al. 2012), with each run of the dataset undergoing 5,000,000 generations, sampling every 1000 generations. The analysis was terminated when the average standard deviation of the split frequency was lower than 0.01, ultimately discarding 25% as burn-in. The output parameter files of each run were checked in TRACER v1.7.1 to ensure that the effective sample size (ESS) values for each parameter were greater than 200 (Rambaut et al. 2018). Briefly, the genetic distances of COI were calculated using MEGA 6.06 under the Kimura 2-parameter substitution model (Lázaro et al. 2009; Solà et al. 2013; Tamura et al. 2013; Wang et al. 2024). Unidentified Asian species were excluded from the genetic distance analysis.

Abbreviations used in the figures

b: bump; **bc**: bursal canal; **ca**: common atrium; **cb**: copulatory bursa; **cg**: cement glands; **cpg**: cyanophil penis glands; **coa**: copulatory apparatus; **d**: diaphragm; **du**: duct; **ed**: ejaculatory duct; **epg**: erythrophil penis glands; **e**: eye; go: gonopore; **lod**: left oviduct; **lvd**: left vas deferens; **ma**: male atrium; **od**: oviduct; **ph**: pharynx; **pp**: penis papilla; **rod**: right oviduct; **rvd**: right vas deferens; **sg**: shell glands; **sph**: spermatophore; **sv**: seminal vesicle; **vd**: vas deferens.

Table 1. GenBank accession numbers of sequences for species taxa used in the phylogenetic analyses.

Species	GenBank			
	COI	***ITS–1***	***28S***	***18S***
D. aconcinna	PV055688	PV055833	PV055834	–
D. adunca	OL505739	OL527659	–	–
D. aethiopica	KY498845	KY498785	KY498806	KY498822
D. afromontana	KY498846	KY498786	KY498807	KY498823
D. ancoraria	OR326966	OR296750	OR225689	OR198141
D. arabica	OL410620	OK587374	OK491342	OK646637
D. arcadia	KC006971	KC007044	OK491318	KF308694
D. ariadnae	KC006972	KC007048	OK491317	OK646636
D. batuensis	OL410626	OK587362	OK491316	OK646630
D. benazzii	FJ646977 + FJ646933	FJ646890	MK712509	OK646628
D. bengalensis	–	FJ646897	–	–
D. bifida	KY498851	KY498791	KY498813	KY498843
D. bijuga	MH119630	–	–	MH113806
D. circumcisa	MZ147041	MZ146782	–	–
D. cretica	KC006976	KC007050	OK491340	KF308697
D. constrictiva	MZ871766	MZ869023	–	–
D. damoae	KF308768	KC007057	OK491310	OK646619
D. deharvengi	KF907820	KF907817	KF907824	–
D. effusa	KF308780	KC007058	OK491311	OK646618
D. elegans	KC006984	KC007063	OK491313	KF308695
D. etrusca	FJ646984 + FJ646939	FJ646898	OK491312	OK646617
D. gemmulata	OL632201	–	–	–
D. gibberosa	KY498857	KY498803	KY498819	KY498842
D. gonocephala	FJ646986+FJ646941	FJ646901	DQ665965	DQ666002
D. granosa	OL410634	KY498795	KY498816	KY498833
D. hepta	MK712639	MK713035	OK491309	OK646612
D. hoidi	OR650791	–	–	–
D. improvisa	KC006987	KC007065	OK491304	KF308696
D. japonica	FJ646990	FJ646904	DQ665966	D83382
D. liguriensis	OL410632	OK587358	OK491353	OK646615
D. malickyi	KC006988	KC007068	OK491294	OK646585
D. majuscula	MW533425	MW533591	–	–
D. mariae	OR650829	–	–	–
D. musculosa	OR189184	OR205922	–	–
D. naiadis	KF308756	OK587343	OK491293	–
D. notogaea	FJ646993+FJ646945	FJ646908	KJ599720	KJ599713
D. parasagitta	KF308739	KC007073	–	OK646577
*D. patula**	PV786826	PV788696	PV788698	PV788697
D. pendula	OR195337	OR205921	–	–
*D. postica**	PV786825	PV788693	PV788694	PV788695
D. pustulata	MH119631	OK587366	OK491355	MH113807
D. ryukyuensis	AB618488	FJ646910	OK491323	AF050433
D. saccata	PV055687	PV055830	PV055832	PV055831
D. sagitta	KC007006	KC007077	OK491320	OK646567
D. semiglobosa	MW525210	MW526992	–	–
D. sicula	KF308797	OK587339	OK491287	KF308693
D. sigmoides	KY498849	KY498789	KY498811	KY498827
D. sinensis	KP401592	–	–	–
D. subtentaculata	MK712628	MK713004	MK712501	AF013155
D. tumida	OL505740	OL527709	–	–
D. umbonata	MT176641	MT177211	MT177210	MT177214
D. verrucula	MZ147040	MZ146760	–	–
R. postrema	KF308763	–	MG457274	KF308691
S. mediterranea	JF837062	AF047854	DQ665992	U31085
S. polychroa	FJ646975+FJ647021	–	DQ665993	AF013152
Dugesia sp. twn1 (Dtwn1)#	OL410673	OK587389	OK646554	OK491367
Dugesia sp. twn2 (Dtwn2)#	OL410674	OK587388	OK646553	OK491366

Species	GenBank			
	COI	*ITS–1*	*28S*	*18S*
Dugesia sp. twn3 (Dtwn3)#	OL410675	OK587387	OK646552	OK491365
Dugesia sp. jap1 (Djap1)#	OL410644	OK587376	OK646500	OK491328
Dugesia sp. jap2 (Djap2)#	OL410645	OK587367	OK646599	OK491330
Dugesia sp. jap3 (Djap3)#	OL410646	OK587375	OK646598	OK491329
Dugesia sp. jap4 (Djap4)#	OL410647	OK587350	OK646597	OK491303
Dugesia sp. jap5 (Djap5)#	OL410648	OK587344	OK646596	OK491284
Dugesia sp. ryu1 (Dryu1)#	OL410662	OK587379	OK646571	OK491322
Dugesia sp. ryu2 (Dryu2)#	OL410663	OK587378	OK646570	OK491323
Dugesia sp. ryu3 (Dryu3)#	OL410664	OK587377	OK646569	OK491324
Dugesia sp. ino (Dino)#	–	OK587356	OK646606	OK491337
Dugesia sp. ind (Dind)#	OL410638	OK587357	OK646607	OK491338
Dugesia sp. tai (Dtai)#	OL410668	OK587373	OK646562	OK491286
Dugesia sp. ban (Dban)#	OL410625	OK587393	OK646631	OK491360

* the new specis of this study.
# unidentified *Dugesia* specimens sequences from Asia used for phylogenetic analyses of Asia species (Solà et al. 2022).

Data availability

The authors declare that the data supporting the findings of this study are available within the paper and its Supplementary Information files. Should any raw data files be needed in another format, they are available from the corresponding author upon reasonable request.

Results

Molecular phylogeny and genetic distances

None of the three specimens of each of the two new species described here, *Dugesia postica* and *D. patula*, displayed any variation in their molecular sequences. The phylogenetic trees generated from the concatenated dataset of four genes using Bayesian inference (BI) and maximum likelihood (ML) analyses displayed nearly identical topologies, differing only in a few branches and support values (Fig. 2; Suppl. material 1: fig. S1). In our single-gene phylogenetic trees, the two new species formed distinct clades that did not cluster with any other *Dugesia* species included in our molecular analyses (Suppl. material 1: figs S2–S5).

In our phylogenetic analysis, the clade formed by the Afrotropical/Mediterranean and Malagasy sister groups (Fig. 2; pp = 0.96, bs = 87) was the sister taxon to various phylo-biogeographic clades, including species from Cameroon, the Western Palearctic, the Oriental/Australasian, and the Eastern Palearctic/Oriental regions (Fig. 2; pp = 1.00, bs = 100). Within the latter clade, the Western Palearctic group forms a distinct subclade (Fig. 2; pp = 1.00, bs = 100), while together species from the Oriental/Australasian, Eastern Palearctic/Oriental I, and Eastern Palearctic/Oriental II groups form another subclade (Fig. 2; pp = 1.00, bs = 93). The two new species described in the present study, *D. postica* and *D. patula*, share a sister-group relationship with high support (Fig. 2; pp = 1.00, bs = 100) and fall within the Eastern Palearctic/Oriental I subclade.

The highest COI distance values between *D. postica* and *D. patula* and their congeners were 24.10% and 22.86% with *D. arabica* Harrath & Sluys, 2013 and *D. naiadis* Sluys, 2013, respectively. Additionally, the maximum ITS-1 distances of *D. postica* and *D. patula* from their congeners were 22.63% and 22.17% (both with respect to *D. pustulata* Harrath & Sluys, 2019), respectively. The minimum genetic distances observed among all congeners were 9.01% for COI and 2.41% for ITS-1, both occurring between *D. postica* and *D. patula* (Suppl. material 2).

Systematic account

Order Tricladida Lang, 1884
Suborder Continenticola Carranza, Littlewood, Clough, Ruiz-Trillo, Baguñà & Riutort, 1998
Family Dugesiidae Ball, 1974
Genus *Dugesia* Girard, 1850

***Dugesia patula* Chen & Dong, sp. nov.**
https://zoobank.org/36826FE2-FAE9-47BF-ADC9-85A77379C82B

Habitat and reproduction. The specimens were collected from Yulong County, at the foot of Yulong Snow Mountain, at an elevation of 1730 m. The ambient temperature was 24.8 °C, with the water temperature being 16.4 °C. The Jinsha Jiang river is a broad and fast-flowing course, with murky water and a bottom rich in mud and sand (Fig. 3A). In the field, flatworms could be seen freely crawling on the surface of the mud and sand. All observed flatworms were asexual individuals. Under laboratory conditions and after two months of cultivation, the asexual worms were fissiparous, of which 8 ex-fissiparous specimens sexualized (Fig. 3B). However, after two years of breeding in the laboratory, no cocoons were observed.

Material examined. *Holotype*: ZMHNU–LMYL4, Yulong County, Lijiang City, Yunnan Province, China, 27°9'26"N, 99°48'25"E, 17 June 2023, coll. G-W Chen, Z-M Dong, and coworkers, sagittal sections on 28 slides.

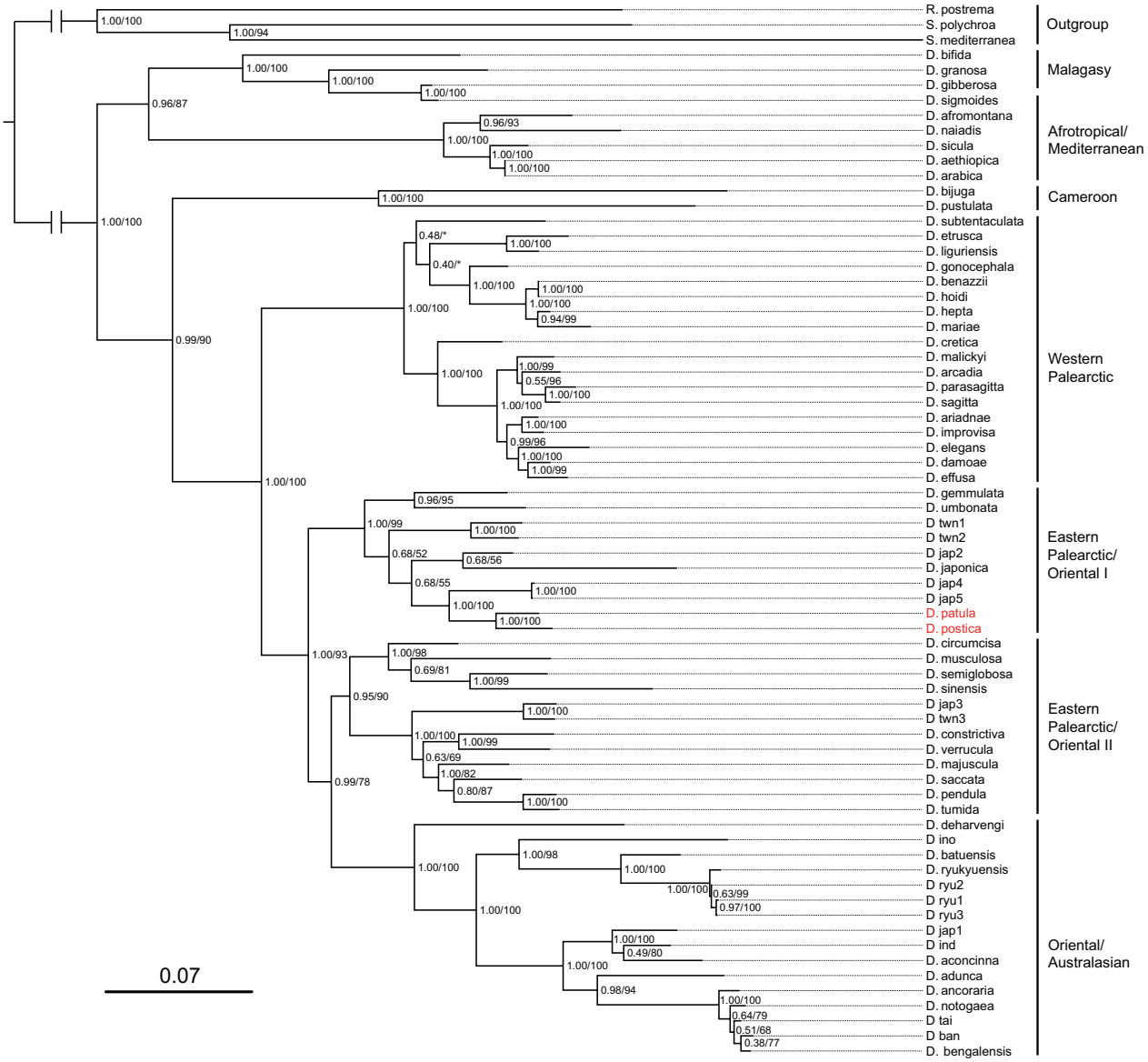

Figure 2. Molecular phylogenetic tree obtained from Bayesian inference of the 18S rDNA, ITS-1, 28S rDNA, and COI concatenated dataset. Numbers at nodes indicate support values (posterior probability/bootstrap). New species indicated in red. Scale bar: substitutions per site.

***Paratypes*:** ZMHNU–LMYL2, 3, and 7 ibid., sagittal sections on 60, 49, and 27 slides, respectively; RMNH.VER.22274.1, ibid., sagittal sections on 30 slides; RMNH.VER.22274.2, ibid., sagittal sections on 20 slides; ZMHNU–LMYL5, ibid., transverse sections on 42 slides; ZMHNU–LMYL6, ibid., horizontal sections on 22 slides.

Etymology. The specific epithet is derived from the Latin adjective *patulus*, meaning "spread out," "broad," or "wide open," and alludes to the very broad ejaculatory duct and its wide opening at the tip of the broad and blunt penis papilla.

Diagnosis. *Dugesia patula* is characterized by the following features: symmetrical openings of the oviducts into the bursal canal; vasa deferentia opening symmetrically into the mid-lateral portion of the seminal vesicle; a large and pointed diaphragm; a short duct between the seminal vesicle and diaphragm; a very broad and short ejaculatory duct opening at the tip of the penis papilla.

Description. Living sexual animals measured 13.8–18.7 mm in length and 2.1–3.3 mm in width; asexual worms measured 7.3–12.4 mm in length and 1.37–1.72 mm in width. The head is bluntly triangular and provided with two blunt auricles and two eyes located within pigment-free patches. The dorsal body surface is brown, with lighter brown body margins (Fig. 3B); the ventral body surface is light brown.

The pharynx is located in the middle of the body, measuring approximately one-sixth of the body length (Fig. 3B). The mouth opening is located on the ventral side at the posterior end of the pharyngeal pocket. The outer pharyngeal musculature is composed of a subepithelial layer of longitudinal muscles, followed by a thin layer of circular muscles. The inner pharyngeal musculature

Figure 3. *Dugesia patula*. **A.** Sampling site and habitat; **B.** Sexually mature, live individual. Scale bar: 2 mm

consists of a thick subepithelial layer of circular muscle, followed by a thin layer of longitudinal muscle.

The ovaries are located at a short distance behind the brain, i.e., between 1/10th and 1/14th of the distance from the brain to the root of the pharynx. The oval-shaped ovaries occupy about one-third of the dorso-ventral space. From the dorsal sides of the ovaries, the oviducts extend posteriorly along the ventral side up to the level of the gonopore, after which they curve dorso-medially to open separately and symmetrically into the ventro-lateral portion of the bursal canal, at the point where the canal communicates with the common genital atrium (Figs 4A, 5). Cyanophil shell glands discharge their secretion into the vaginal region of the bursal canal, immediately ventrally of the oviducal openings (Figs 4A, 5).

The large, sac-shaped copulatory bursa is located far behind the pharynx (at approximately 400–600 µm behind the pharyngeal pocket) and occupies the entire dorso-ventral space. Its length is about twice the dorso-ventral diameter of the body, i.e., measuring approximately 600–800 µm (Fig. 4B). Furthermore, there is a considerable distance between the bursa and the penis bulb (Fig. 5), with the consequence that the bursal canal is rather long. The bursa is lined by a stratified, columnar, vacuolated epithelium provided with basal nuclei and is devoid of any surrounding musculature (Fig. 4B). The rather broad bursal canal arises from the mid-posterior wall of the copulatory bursa, from where it runs posteriad, curving downwards at the level of the gonopore to open into the common atrium (Figs 4C, D, 5). The bursal canal is lined with cylindrical, nucleated, ciliated cells and surrounded by a thin, subepithelial layer of longitudinal muscles, followed by a thicker—at least on the ventral side of the canal—layer of circular muscle. There is an extra outer layer of longitudinal musculature extending from the atrium to halfway along the bursal canal, forming the ectal reinforcement.

The dorsal testes occupy about 1/3 of the dorso-ventral space and extend from the rear of the ovaries to the posterior end of the body; the testes house numerous mature spermatozoa.

At the posterior end of the copulatory bursa, the vasa deferentia begin to expand to form spermiducal vesicles, which are packed with sperm (Fig. 5). At the anterior level of the penis bulb, the spermiducal vesicles diminish abruptly in diameter upon curving dorso-medially and, subsequently, penetrating the penis bulb to open symmetrically into the mid-lateral portion of the seminal vesicle (Fig. 5). These narrow portions of the vasa deferentia are lined with cuboidal, nucleated cells and surrounded by a thick layer of circular muscles.

The penis bulb is positioned in the central portion of the body and measures almost half of the dorso-ventral space (Figs 4C–F, 5). A large, sac-shaped seminal vesicle occupies a major portion of the penis bulb. The vesicle is lined by a flat, nucleated epithelium and is surrounded by a thick layer of irregularly crosswise arranged muscle fibers that fills a major portion of the penis bulb (Fig. 4E, F). The postero-ventral portion of the seminal vesicle narrows to form a short duct that arises from the posterior wall of the seminal vesicle and opens into a large and pointed diaphragm (Figs 4C–F, 5). This connecting duct is lined with a nucleated epithelium and surrounded by a thin layer of circular muscles. The diaphragm receives the abundant secretion of orange-staining penis glands (Fig. 4C, D). The diaphragm points into a very broad and short ejaculatory duct, which forms a large cavity. The ejaculatory cavity lined with a cuboidal, infranucleated epithelium and is devoid of any well-discernible musculature. The ejaculatory cavity immediately gives rise to a very broad opening at the blunt tip of the penis papilla (Figs 4C–F, 5).

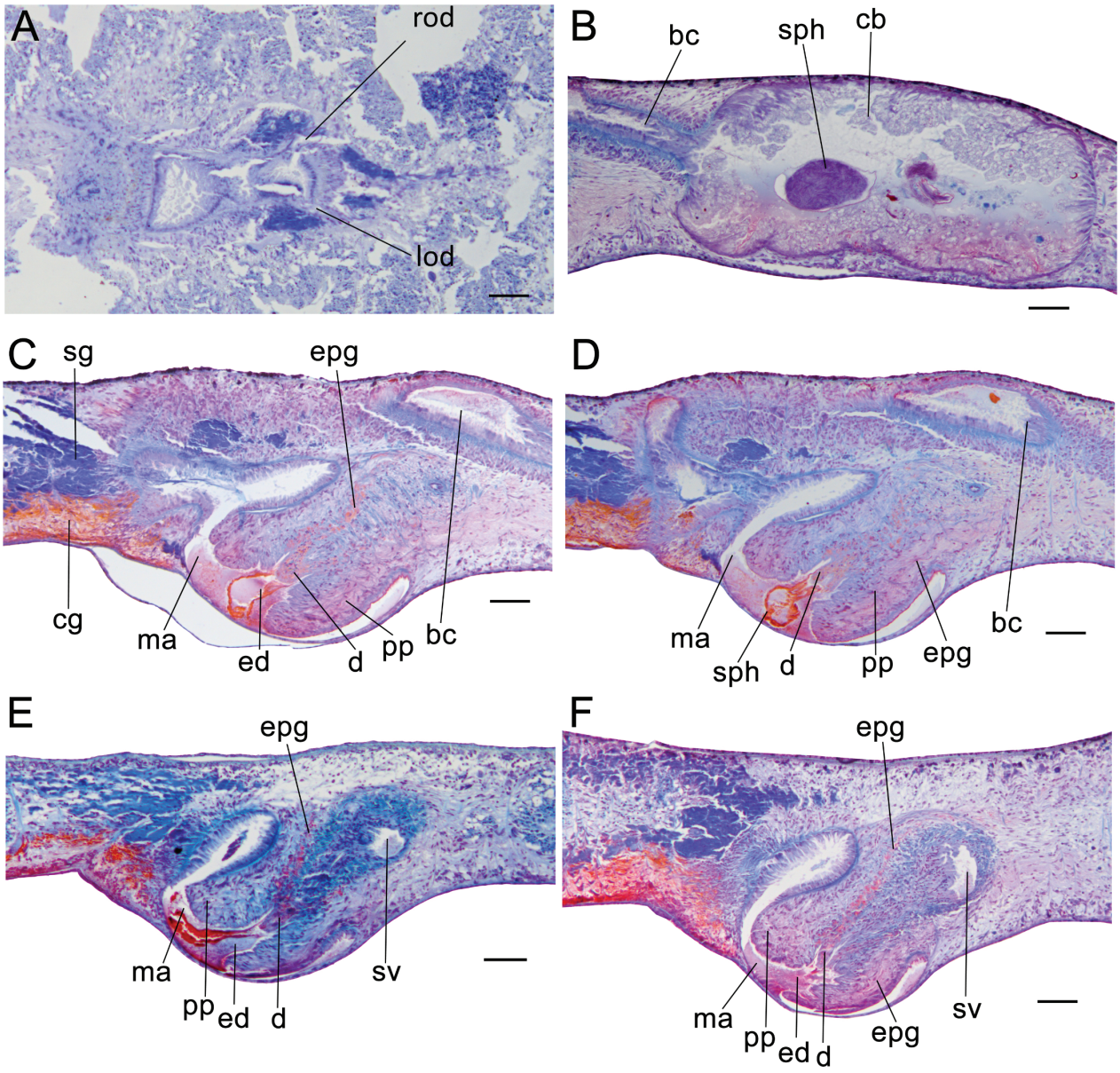

Figure 4. *Dugesia patula*. **A.** Horizontal section of paratype ZMHNU–LMYL6, showing openings of oviducts into bursal canal; **B.** Sagittal section of holotype ZMHNU–LMYL4, showing bursal canal and copulatory bursa with spermatophore; **C.** Sagittal section of holotype ZMHNU–LMYL4, showing ejaculatory duct, diaphragm, and penial glands; **D.** Sagittal section of holotype ZMHNU–LMYL4, showing large, pointed diaphragm and spermatophore; **E.** Sagittal section of paratype ZMHNU–LMYL8, showing ejaculatory duct, seminal vesicle, diaphragm, and penial glands; **F.** Sagittal section of paratype ZMHNU–LMYL3, showing ejaculatory duct, diaphragm, and penial glands. Scale bars: 100 µm

The penis papilla is a barrel-shaped structure, covered with a nucleated epithelium, which is underlain by a subepithelial layer of circular muscle, followed by a layer of longitudinal muscle fibers. A second type of erythrophilic penis glands discharge their sections through the blunt tip of the papilla. The glandular elements of this second type of penial gland lie far outside of the penis bulb (Figs 4C, D, F, 5) and produce a more finely granular secretion than those opening into the diaphragm.

The rather spacious male atrium narrows to form a short canal that opens into the common atrium, the latter leading to a gonoduct, which opens through the ventral gonopore; the gonoduct is lined by a tall, columnar, nucleated epithelium and receives the openings of abundant, erythrophilic cement glands (Figs 4C–F, 5).

In several specimens, a sclerotic spermatophore is present in the ejaculatory duct or in the copulatory bursa (Fig. 4B, D).

Discussion. The presence of an extremely wide-mouthed opening of the ejaculatory duct at the tip of the penis papilla sets *Dugesia patula* immediately apart from its congeners, as for none of the presently known species has such a wide opening been reported. There are only two species that have relatively wide openings of their ejaculatory ducts, albeit considerably less wide than in *D. patula*, viz., *D. afromontana* Stocchino & Sluys, 2012 and *D. musculosa* Chen &

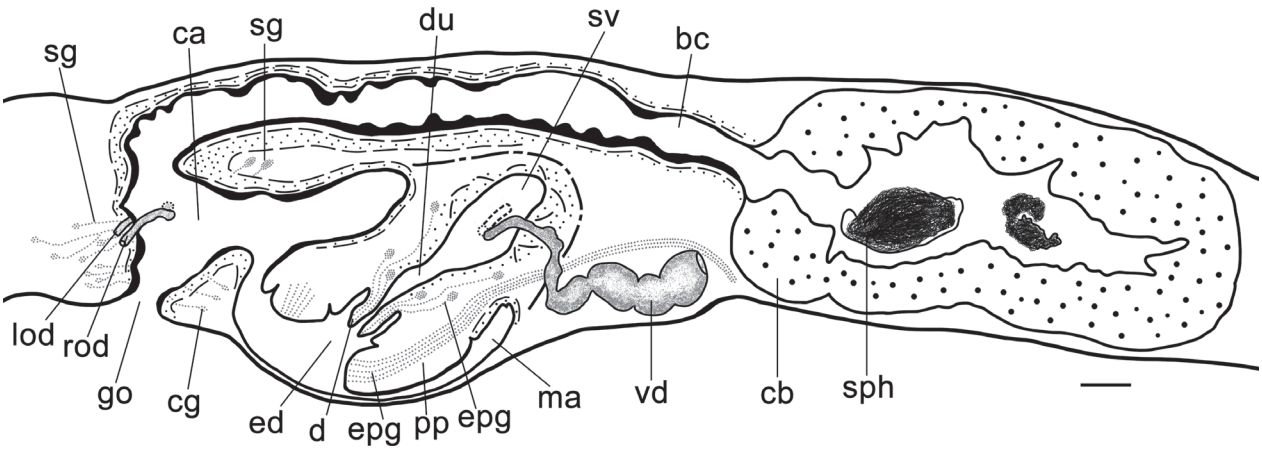

Figure 5. *Dugesia patula*. Sagittal reconstruction of the copulatory apparatus of holotype ZMHNU–LMYL4. Scale bar: 100 µm

Dong, 2024 (Stocchino et al. 2012; Wang et al. 2024). However, in other characters, *D. patula* is rather different from either of these two congeners. For example, in *D. afromontana* the oviducts open asymmetrically into the bursal canal, the seminal vesicle is elongated, and the diaphragm is stubby, contrasting with conditions in *D. patula*. The latter is here reported from Yunnan Province, while *D. musculosa* is known from an adjacent province in China, Guangxi Province. Despite this geographic proximity, there are considerable anatomical differences between both species. Notably, *D. musculosa* exhibits (a) a highly muscular bursal canal, (b) a large, rounded seminal vesicle that receives the asymmetrical openings of the vasa deferentia, and (c) a stubby diaphragm, features that are all absent in *D. patula*. In *D. musculosa* the copulatory bursa is also rather large, as in *D. patula*, but in contrast to the latter, its bursa is situated directly in front of the penis bulb. It is noteworthy that a large copulatory bursa is present also in *D. bursagrossa* Harrath & Sluys, 2025, from Saudi Arabia. But in this species the bursa is extremely large, while it is also located immediately anterior to the penis bulb (cf. Harrath et al. 2025, Fig. 7). Furthermore, in *D. bursagrossa* the ejaculatory duct opens subterminally at the penis papilla, contrasting with the wide, terminal opening in *D. patula*.

The available molecular data also support the conclusion that *D. patula* is different from *D. afromontana* and *D. musculosa* (Fig. 2, Suppl. materials 2, 3).

Another noteworthy feature of *D. patula* concerns its large and pointed diaphragm. Until recently, such a pointed diaphragm was known only from *Dugesia* species from the Western Palearctic region: *D. cretica* (Meixner, 1928), *D. gonocephala* (Dugès, 1830), *D. liguriensis* De Vries, 1988, *D. minotauros* De Vries, 1984, *D. praecaucasica*, *D. transcaucasica*, and *D. leporii* Pala, Stocchino, Corso & Casu, 2000 (Stocchino et al. 2017). However, it turned out to be present also in *D. crassimentula* Sluys & Stocchino, 2024, and *D. insolita* Stocchino & Sluys, 2024, from Madagascar (Stocchino et al. 2024), albeit in the last-mentioned species, the diaphragm has taken over the function of the penis papilla. Thus, *D. patula* is the first species from the Oriental Region for which a pointed diaphragm is reported.

Dugesia postica Chen & Dong, sp. nov.

https://zoobank.org/44F519BC-00D7-4746-A4D6-39C623C659B1

Habitat and reproduction. Specimens were collected from Butterfly Spring, Dali City, at an elevation of 1980 m and a water temperature of 15 °C, where the planarians inhabit small pools formed by spring water and a large number of free-roaming planarians could be observed (Figs 1, 6A, C). In the field, sexually mature individuals were observed, as well as one yellow cocoon attached to a stone, which turned from yellow to black within 2 to 3 days. Under laboratory conditions, after approximately 60 days of culturing, 6 ex-fissiparous individuals sexualized and were capable of laying cocoons. The cocoons were spherical in shape (about 1 mm in diameter) and provided with a stalk (Fig. 6D, E). However, to date, neither cocoons collected from the wild nor those produced in the laboratory have hatched, suggesting that they are infertile.

Material examined. ***Holotype*:** ZMHNU–NJWS4, Butterfly Spring, Dali City, Yunnan Province, China (25°54'33"N, 100°5'41"E), 6 October 2019, coll. G-W Chen, Z-M Dong, and coworkers, sagittal sections on 14 slides.

***Paratypes*:** ZMHNU–NJWS1, 2, 5, 6, ibid., sagittal sections on 32, 51, 14, and 38 slides, respectively; RMNH.VER.22273.1, ibid., sagittal sections on 12 slides; RMNH.VER.22273.2, ibid., sagittal sections on 16 slides; ZMHNU–NJWS8 and 10, ibid., transverse sections on 32 and 41 slides; ZMHNU–NJWS7, ibid., horizontal sections on 7 slides.

Etymology. The specific epithet is derived from the Latin adjective *posticus*, behind or placed after, referring to the diaphragm being displaced towards the terminal part of the penis papilla.

Diagnosis. *Dugesia postica* is characterized by the following features: symmetrical openings of the oviducts into the bursal canal; comparatively long bursal canal; broad penis papilla; generally with a slightly asymmetrical penis papilla, with a somewhat larger dorsal lip as compared with the ventral one; penis papilla with a small, dorsal bulge; a long connecting duct between the seminal vesicle and diaphragm; small diaphragm displaced towards the tip of the penis papilla; short ejaculatory duct

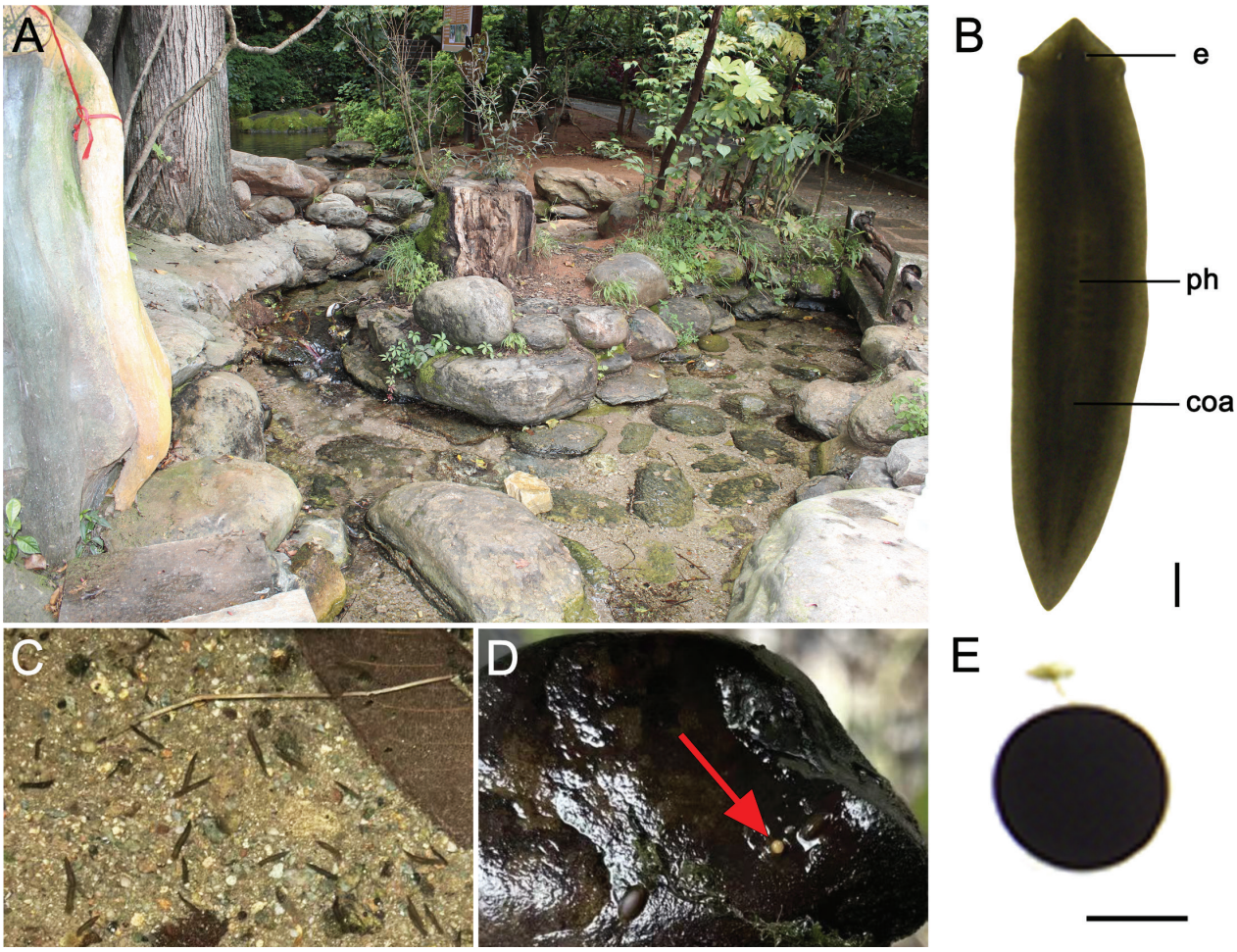

Figure 6. Habitat and external appearance of *Dugesia postica*. **A.** Sampling site and habitat; **B.** Sexually mature, live individual; **C.** Free-roaming worms; **D.** A yellow cocoon (indicated by a red arrow) attached to a stone; **E.** A cocoon with a stalk. Scale bars: 2 mm (**A, B**); 1 mm (**C–E**).

opening subterminally through the ventral wall of the penial papilla; posterior portion of male atrium forming a relatively long and broad duct that connects with the common genital atrium.

Description. Living, sexual animals measured 12.1–14.5 mm in length and 2.3–3.8 mm in width; asexual worms measured 9.7–11.6 mm in length and 1.6–1.9 mm in width. The head is bluntly triangular and provided with two short auricles and two eyes located within pigment-free spots. The dorsal colour is dark charcoal, with the edges being lighter, while the ventral surface is light grey (Fig. 6B). The pharynx is positioned in the middle of the body, measuring approximately one-sixth of the body length (Fig. 6B). The outer pharyngeal musculature is composed of a subepithelial layer of longitudinal muscles, followed by a thin layer of circular muscles. The inner pharyngeal musculature consists of a subepithelial and thick layer of circular muscle, followed by a thin layer of longitudinal muscle. The mouth opening is situated at the hind end of the pharyngeal pocket.

The ovaries are oval, occupying about one-third of the dorso-ventral space. The ovaries are located at a considerable distance behind the brain, i.e., at approximately 1/4th of the distance between the brain and the root of the pharynx. From the ovaries, the infranucleated oviducts originate at the postero-dorsal wall of the ovaries and run ventrally in a caudal direction to the level of the gonopore. Hereafter, the oviducts curve dorso-medially to open symmetrically into the anterior portion of that part of bursal canal where the canal communicates with the common genital atrium (Fig. 7A). Cyanophil shell glands discharge their secretion into the vaginal region of the bursal canal, immediately ventrally to the oviducal openings.

A moderately sized, sac-shaped copulatory bursa is situated immediately posterior to the pharynx and usually at some distance anterior to the penis bulb; the bursa occupies the entire dorso-ventral space (Fig. 7C, E). The bursa is lined by a stratified, columnar, vacuolated epithelium provided with basal nuclei and is devoid of any surrounding musculature.

This rather anterior position of the bursa, combined with the posterior portion of male atrium that forms a relatively long and broad duct, which connects with the posteriorly displaced common genital atrium, makes the bursal canal comparatively long. It runs backwards, more

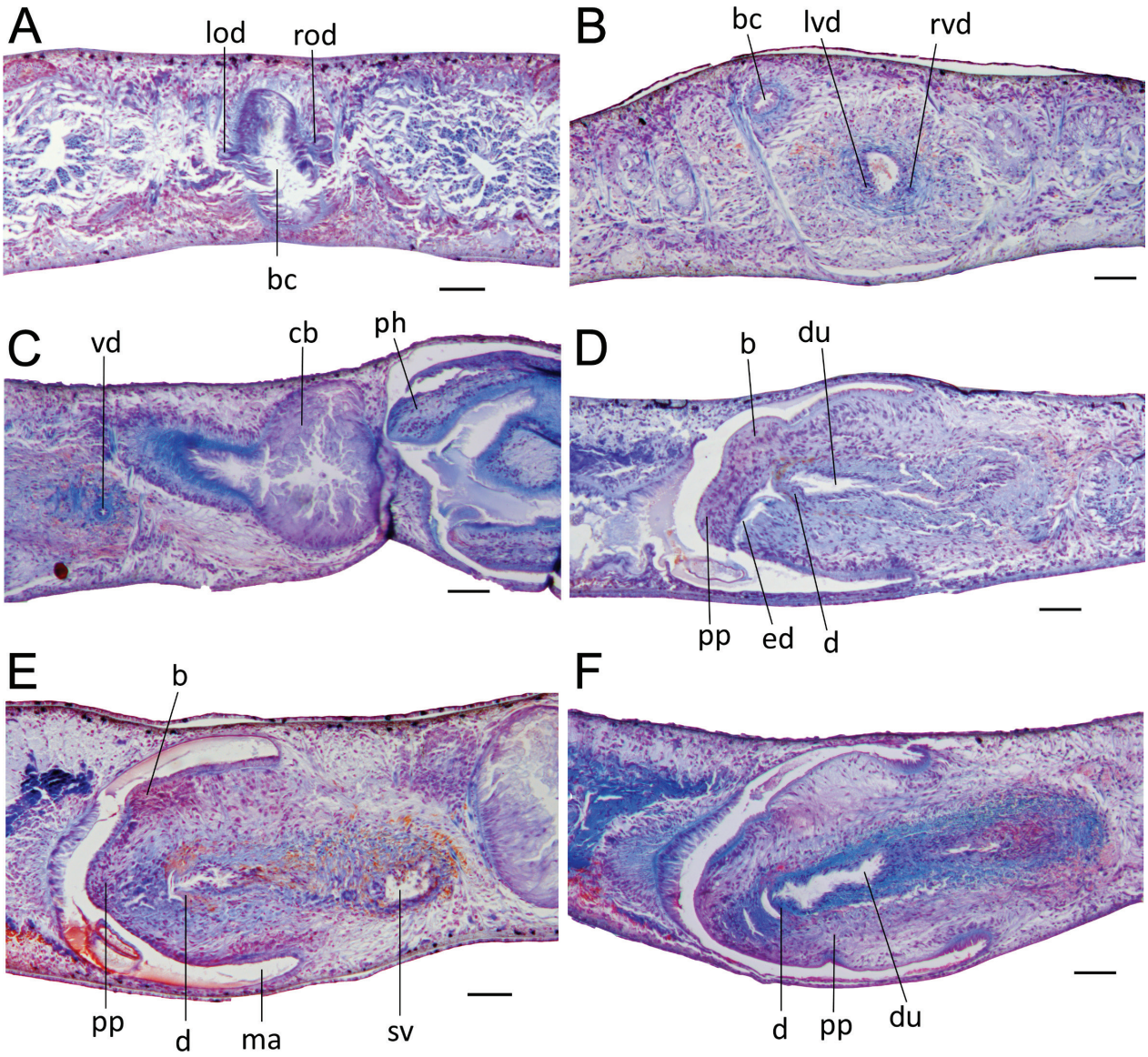

Figure 7. *Dugesia postica*. **A.** Transverse section of paratype ZMHNU–NJWS11, showing symmetrical openings of oviducts into bursal canal; **B.** Transverse section of paratype ZMHNU–NJWS8, showing vasa deferentia and seminal vesicle; **C.** Sagittal section of paratype ZMHNU–NJWS3, showing the location where the bursal canal connects to the copulatory bursa and the copulatory bursa directly behind the pharynx; **D.** Sagittal section of paratype ZMHNU–NJWS1, showing bump on penis papilla, diaphragm, and ejaculatory duct; **E.** Sagittal section of holotype ZMHNU–NJWS4, showing bump on penis papilla, diaphragm, and seminal vesicle; **F.** Sagittal section of paratype ZMHNU–NJWS3, showing diaphragm and ejaculatory duct. Scale bars: 100 μm

or less parallel to the body surfaces, while at the level of the gonopore it bends downwards to open into the common atrium. The bursal canal is lined with cylindrical, nucleated, ciliated cells and surrounded by a subepithelial layer of longitudinal muscles, followed by a layer of circular muscle. There is an extra outer layer of longitudinal musculature extending from the atrium to halfway along the bursal canal, forming the ectal reinforcement.

The mature testes, provided with numerous spermatozoa, are situated dorsally and extend from the rear of the ovaries to the posterior end of the body. At the level of the copulatory bursa, the vasa deferentia expand to form spermiducal vesicles, which are packed with sperm. At the level of the penis bulb, the vasa deferentia curve dorso-medially, decrease considerably in diameter, forming narrow ducts, and, subsequently, penetrate the penis bulb to open symmetrically into the posterior portion of the seminal vesicle (Fig. 7B). The sperm ducts are lined with nucleated cells and surrounded by a layer of circular muscles.

The penis bulb occupies about one-half of the dorso-ventral space (Figs 7D–F, 8, 9) and houses a small, oval-shaped or globular seminal vesicle, which is lined by a flat, nucleated epithelium and surrounded by a layer of irregularly crosswise arranged muscle fibers (Fig. 7D–F). From the posterior wall of the seminal vesicle arises a comparatively broad and long connecting duct that opens into a rather small and stubby diaphragm (Fig. 7D). This connecting duct is lined with a nucleated epithelium and surrounded by several layers of thin circular muscles. Seminal vesicle and connecting duct receive the openings

of orange-staining penial glands. The diaphragm points into the short ejaculatory duct, which curves abruptly downwards to open subterminally through the ventral wall of the penis papilla. The diaphragm receives the abundant secretion of erythrophil penis glands (Fig. 7D–F). The ejaculatory duct is lined with a cuboidal, infranucleated epithelium and is devoid of any discernible musculature. Cyanophil penis glands discharge their secretion into the ejaculatory duct (Fig. 7D, E). A spermatophore is present in the ejaculatory duct and/or the male atrium of the specimens NJWS1, NJWS2, NJWS4, and NJWS6.

The penis papilla is a rather broad structure, which is somewhat asymmetrical in that it has a slightly larger dorsal lip as compared with the ventral one. This condition is due to the slightly ventrally displaced position of the seminal vesicle and the equally displaced course of the connecting duct. The asymmetrical condition is only weakly expressed in the paratypes ZMHNU–NJWS1 and NJWS2 but more strongly present in holotype NJWS4 and paratype NJWS6 (Figs 8, 9). The papilla is characterized by a bulge or bump on its dorsal wall, where erythrophilic glands discharge their secretion to the exterior. The penis papilla is lined with a nucleated epithelium, which is underlain by a subepithelial layer of circular muscle, followed by a layer of longitudinal muscle fibers (Figs 7D, 8, 9).

The penis papilla fills almost the entire anterior portion of the male atrium, but the posterior portion of male atrium forms a relatively long and broad duct that connects with the common genital atrium. The male atrium is lined with a cuboidal, nucleated epithelium. The common atrium communicates with the gonoduct, which leads to the ventral gonopore; the gonoduct is lined by a tall, columnar epithelium and receives the openings of abundant cement glands (Figs 7F, 8, 9).

Discussion. A centrally or ventrally displaced course of the ejaculatory duct and a terminal or subterminal opening of the ejaculatory duct at the tip of the penis papilla form important taxonomic characters in the identification of species of *Dugesia* and for resolution of phylogenetic relationships within the genus (cf. Sluys et al. 1998; Stocchino et al. 2017). Another important character concerns the absence or presence of a duct intercalated between the seminal vesicle and the diaphragm (character state 5–1 in Sluys et al. 1998). With respect to these three characters, *D. postica* exhibits the combination of character states concerning a ventrally displaced ejaculatory duct (i.e., an asymmetrical penis papilla), a subterminal ventral opening of the ejaculatory duct, and a duct (either long or short) connecting the diaphragm with the seminal vesicle. In this context it is important to realize that a subterminal opening of the ejaculatory duct does not necessarily imply that the penis papilla is asymmetrical, since

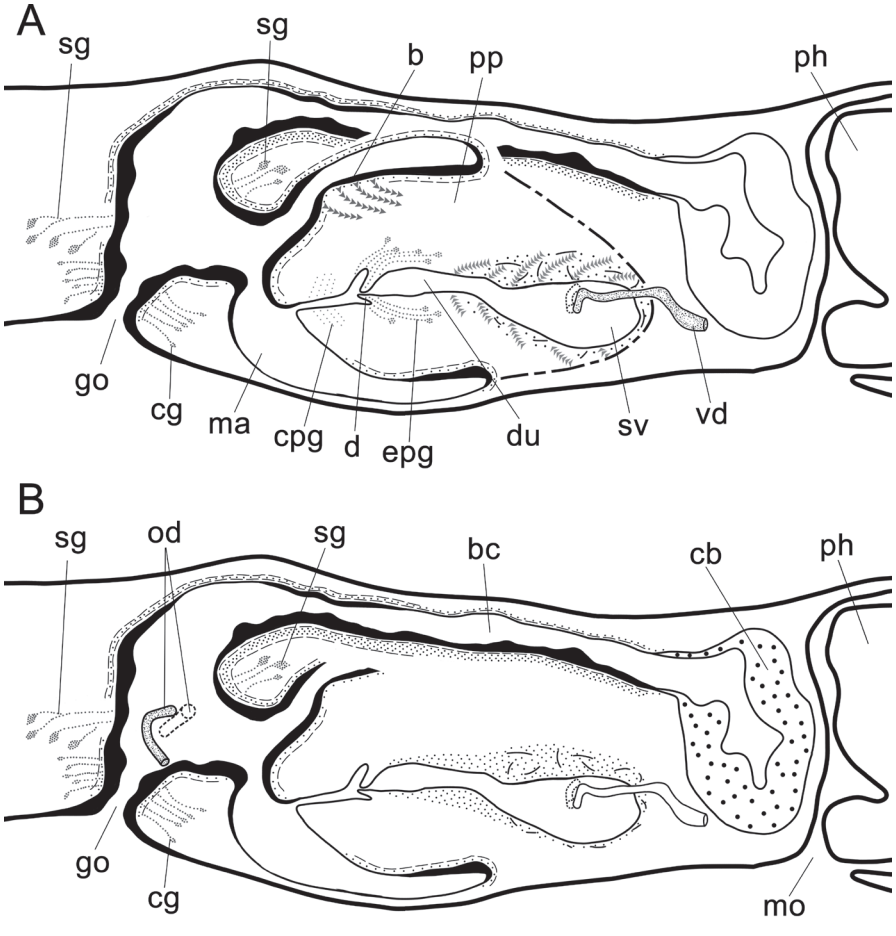

Figure 8. *Dugesia postica*. Sagittal reconstruction of the copulatory apparatus of holotype ZMHNU–NJWS4. **A.** Male copulatory apparatus; **B.** Female copulatory apparatus. Scale bars: 100 μm

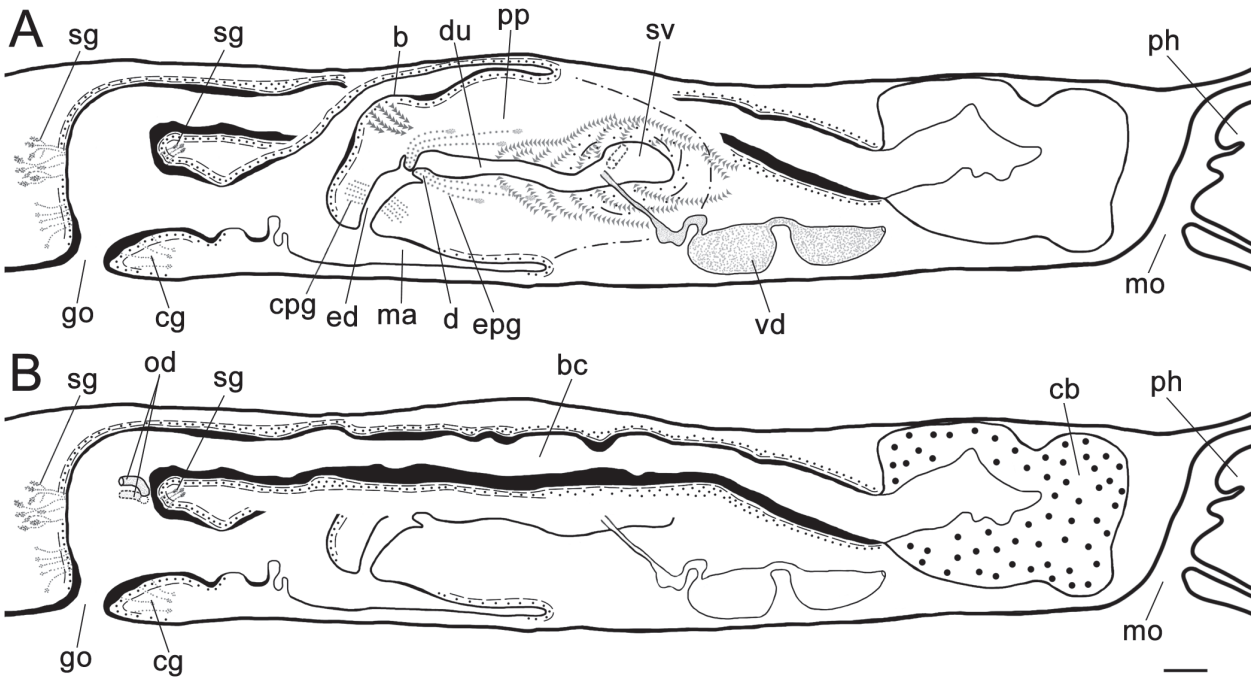

Figure 9. *Dugesia postica*. Sagittal reconstruction of the copulatory apparatus of paratype ZMHNU–NJWS1. **A.** Male copulatory apparatus; **B.** Female copulatory apparatus. Scale bars: 100 µm

the latter condition is defined by the ventrally or dorsally displaced course of the ejaculatory duct at the level of the root of the penis papilla (cf. Stocchino et al. 2017).

The combination of these three character states (ventrally displaced ejaculatory duct, subterminal opening ejaculatory duct, and interconnecting duct between diaphragm and seminal vesicle) is also present in the following species: *D. adunca* Chen & Sluys, 2022; *D. ancoraria* Zhu & Wang, 2024; *D. andamanensis* (Kaburaki, 1925); *D. austroasiatica* Kawakatsu, 1985; *D. batuensis* Ball, 1970; *D. bengalensis*; *D. deharvengi* Kawakatsu & Mitchell, 1989; *D. gemmulata*; *D. japonica* Ichikawa & Kawakatsu, 1964; *D. lindbergi* De Beauchamp, 1959; *D. novaguineana* Kawakatsu, 1976; *D. tamilensis* Kawakatsu, 1980; and *D. verrucula* Chen & Dong, 2021 (Sluys et al. 1998; Wang et al. 2021; Zhu et al. 2024; Chen et al. 2022; Liu et al. 2022b; Ichikawa and Kawakatsu 1964; Kawakatsu et al. 1985; Kawakatsu and Mitchell 1989). However, *D. postica* differs from all of these congeners in several respects.

For example, the symmetrical openings of the oviducts into the bursal canal in *D. postica* contrast with the asymmetrical openings in *D. adunca*, *D. ancoraria*, *D. gemmulata*, and *D. verrucula*. Further, in *D. andamanensis* and *D. deharvengi* the oviducts fuse to form a common oviduct that opens into the bursal canal, in contrast to the separate openings in *D. postica*, while in *D. lindbergi* the oviducts (which open symmetrically into the bursal canal) may sometimes unite to form a very short common oviduct. *Dugesia batuensis* possesses a penial valve, which is absent in *D. postica*. In *D. japonica*, the vaginal region is surrounded by a hump of mesenchymal tissue traversed by several rows of longitudinal and circular muscle fibers, which is absent in *D. postica*. In *D. bengalensis* the vasa deferentia open through the roof of the seminal vesicle, while the ectal reinforcement around the bursal canal extends up to the copulatory bursa, both conditions being different in *D. postica*. The ectal reinforcement layer of *D. lanzai* also extends up to the bursa, while it also has an elongated seminal vesicle that differs from the small and rounded vesicle in *D. postica*. *Dugesia novaguineana* shows the following features, which are all different from the situation in *D. postica*: (a) large, hemispherical penis bulb; (b) large, ovoid seminal vesicle; (c) stubby penis papilla; and (d) the posterior half of the bursal canal being provided with a thick coat of muscles.

Interestingly, *D. ancoraria*, *D. austroasiatica*, *D. tamilensis*, and *D. verrucula* all have a kind of dorsal bump on the penis papilla, as is the case also in *D. postica*. In the above it was already shown that *D. postica* anatomically differs from *D. ancoraria* and *D. verrucula*, notably with respect to the oviducal openings into the bursal canal, despite the presence of a penial bump in these three species. However, anatomical differences between *D. postica* on the one hand and *D. austroasiatica* and *D. tamilensis* on the other hand are more difficult to discern. In both *D. austroasiatica* and *D. tamilensis* the ectal reinforcement muscle layer around the bursal canal does not reach up to the bursa, as is the case also in *D. postica*. It could be argued that in *D. tamilensis* (a) the seminal vesicle is considerably larger, (b) the connecting duct between seminal vesicle and diaphragm is shorter (and thus the diaphragm not displaced towards the tip of the penis papilla), and (c) the ejaculatory duct has a much more extremely subterminal opening, situated near the root of the penis papilla, all being conditions that differ from those in *D. postica*. In *D. austroasiatica* the seminal vesicle is indeed also rather large, in contrast to the small vesicle in *D. postica*. A striking similarity between *D. postica* and *D. austroasiatica* concerns the fact that in

the latter the penial bump or fold also receives the openings of many erythrophilic gland ducts, while its ejaculatory duct also receives abundant secretion of penial glands (cf. Kawakatsu et al. 1985, Fig. 3A, D; Kawakatsu et al. 1986, Fig. 3). It is noteworthy that Kawakatsu et al. (1985, 1986) presumed that *D. austroasiatica* was introduced in Japan from some Southeast Asian country. However, none of the species mentioned above in the comparative discussion, including *D. austroasiatica*, shows the characteristic posteriorly displaced position of the diaphragm, nor the long bursal canal or the long and broad duct connecting male and common atrium, as present in *D. postica*.

Unfortunately, for not all of the *Dugesia* species discussed above is molecular information available, and therefore they could not be incorporated into our analyses. However, *D. adunca*, *D. ancoraria*, *D. batuensis*, *D. bengalensis*, *D. japonica*, *D. gemmulata*, *D. verrucula*, and *D. deharvengi* could be included in our phylogenetic and molecular distance analyses, which revealed that none of these species is similar to or genetically closely related to *D. postica* (Fig. 2; Suppl. materials 2, 3).

Discussion

In this study, we report two new species for the first time from Yunnan Province, southwest China. They form two independent branches in our phylogenetic tree (Fig. 2), and there are considerable genetic distances between them and other congeneric species (Suppl. materials 2, 3). In addition, each new species is characterized by a unique combination of anatomical features, strongly suggesting their separate specific status.

The mitochondrial gene COI and nuclear genes ITS-1, 18S, and 28S, as well as the concatenated four-gene dataset, consistently recovered the two newly identified species as independent branches with strong statistical support (Fig. 2; Suppl. material 1: figs S1–S5; pp = 1.00, bs ≥ 95). Single-gene phylogenetic trees remain highly effective for species identification, demonstrating high resolution at the species level. Phylogenetic analyses based on nuclear genes further resolved these two species as sister taxa (Suppl. material 1: figs S3–S5; bs ≥ 99), a result congruent with the concatenated dataset (Fig. 2; Suppl. material 1: fig. S1; pp = 1.00, bs = 100). In contrast, the COI gene tree placed the two new species within a clade together with the unidentified terminals Djap4 and Djap5 (Suppl. material 1: fig. S2; bs = 99). This discordance may stem from incomplete lineage sorting of the mitochondrial locus.

Consistent with previous studies, the concatenated four-gene phylogeny robustly supported the Western Palearctic clade, which consistently shared a sister-group relationship with the Oriental, Eastern Palearctic, and Australasian taxa (Fig. 2; Suppl. material 1: fig. S1; pp = 1.00, bs = 100; Solà et al. 2022; Wang et al. 2024). However, our single-gene trees failed to recover stable topologies for these relationships. For instance, in the 28S single-gene tree, the Oriental/Eastern Palearctic/Australasian taxa were not monophyletic, as the Western Palearctic species sat among them, with the Western Palearctic clade sharing a sister-group relationship with the Eastern Palearctic/Oriental II/Australasian group (Suppl. material 1: fig. S4; bs = 89), albeit with low support. A similar non-monophyletic pattern was observed in the ITS-1 single-gene tree (Suppl. material 1: fig. S1). These findings suggest the presence of substantial unsampled diversity in regions separating the Western Palearctic and Oriental/Eastern Palearctic/Australasian groups. The conflicting topologies observed in single-gene trees, as compared with the concatenated dataset, are likely due to homoplasy resulting from rapidly evolving sites. Nevertheless, the overall results underscore the superior topological stability of the concatenated four-gene phylogeny.

Phylogenetic analyses based on the concatenated dataset yielded largely congruent and stable topologies between maximum likelihood (ML) and Bayesian inference (BI), with discrepancies restricted to specific nodes within Western Palearctic lineages. Notably, the inclusion of sequences from specimens collected in Japan, the Ryukyu Islands, Taiwan, Thailand, Bangladesh, India, and Indonesia significantly enhanced nodal support for key clades within the Oriental/Eastern Palearctic/Australasian group, as compared to previous studies (Zhu et al. 2024; Wang et al. 2024). These findings enhance our understanding of the biogeographic relationships within these lineages. Earlier phylogenetic reconstructions experienced difficulties in resolving the relationships among three major subclades: (1) the Eastern Palearctic/Oriental I clade, (2) the Oriental/Australasian clade, and (3) the Eastern Palearctic/Oriental II clade (Fig. 2). For instance, Zhu et al. (2024) recovered the Eastern Palearctic/Oriental I clade and the Eastern Palearctic/Oriental II clade as sharing a weakly supported sister-group relationship (Zhu et al. 2024, Fig. 2; pp = 0.72, bs < 50). Our analyses improved the resolution of these clades. Specifically, Bayesian inference strongly supported a sister-group relationship between the Eastern Palearctic/Oriental II clade and the Oriental/Australasian clade (Fig. 2; pp = 0.99, bs = 78), while the Eastern Palearctic/Oriental I clade was robustly recovered as the sister group of these two clades (Fig. 2; pp = 1.00, bs = 93).

The Eastern Palearctic lineages form two distinct clades (Fig. 2), which implies that there may have been two different dispersal routes via which *Dugesia* species colonized this region. The Eastern Palearctic/Oriental II subclade comprises Palearctic lineages exhibiting close affinities to species from southern China, including *D. majuscula* from Hainan, *D. verrucula* from Guangxi, and *D. tumida* from Guangdong. However, these southern regions are geographically separated from the Eastern Palearctic by the Zhejiang–Fujian Hills. In contrast, the Eastern Palearctic/Oriental I subclade includes lineages closely related to species from southwest China. To date, four *Dugesia* species have been identified in southwest China: *D. gemmulata* from Guizhou, *D. umbonata* from Chongqing, and the two new species, *D. postica* and *D. patula*, from Yunnan—all of which cluster within the Eastern Palearctic/Oriental I subclade. Previous studies have demonstrated that the formation of the Hengduan Mountains resulted from the Indo-Eurasian plate collision (~50 Mya), while rapid uplift during the Miocene (15–5 Mya)

contributed to the development of its distinctive north–south-oriented "parallel ridge–valley system," characterized by alternating deep river valleys and high-elevation ridges (Xing and Ree 2017; Favre et al. 2014). In various animal groups, such as the snow finch complex (*Montifringilla*, *Pyrgilauda*, and *Onychostruthus*), population dispersal has been shown to follow these north–south-oriented valleys (e.g., Nu Jiang and Lancang River), with gene flow intensity being positively correlated with connectivity along fault zones (Qu et al. 2006). Furthermore, Solà et al. (2022) proposed that the dispersal of *Dugesia* into East Asia may have occurred via migration from Africa through the Indian subcontinent, followed by colonization after the Indo-Eurasian collision. Upon reaching East Asia, the ongoing orogenic processes in the Southwestern Mountainous Regions may not only have driven speciation but also facilitated northward expansion into continental interiors. Therefore, we hypothesize that *Dugesia* dispersed from the Oriental into the Eastern Palearctic, likely originating from the southwestern mountains of China and migrating northward via the Qinling–Daba Mountains or the Wuling Mountains. However, species diversity in these critical regions, such as the Southwestern Mountainous Regions, remains severely understudied. Expanding taxon sampling in these understudied regions will be essential for reconstructing and testing the hypothesized dispersal routes of *Dugesia* after its arrival in Asia.

In recent years, increasing research efforts have focused on the southwestern mountains of China in an attempt to uncover the drivers behind its high species diversity. For instance, studies on freshwater crabs have shown that the discrete mountain archipelagos in the eastern Hengduan Mountains act as a "species pump," with the unique and restricted climate of the dry-hot valleys enhancing this effect and playing a key role in shaping the region's aquatic biodiversity (Shi et al. 2023). While earlier studies on *Dugesia* in this area, such as that by Liu (1989), primarily addressed morphological descriptions and seasonal patterns of sexualization, the present study is the first to document two new species from the Hengduan Mountains, highlighting the region's potential for undiscovered diversity. Despite these findings, the southwestern mountains of China—recognized as one of the world's biodiversity hotspots—remain underexplored. The species discovered so far are limited in number and unrepresentative of the region's biodiversity, underscoring the urgent need for further, in-depth investigations.

Acknowledgements

This work was supported by the National Natural Science Foundation of China (grant numbers: 32270501, 32470463, 32200376), the Major Public Welfare Project of Henan Province (grant number: 201300311700), the Postdoctoral Research Project of Henan Province (grant number: HN2022136), the Foundation for the Key Research Program of Higher Education of Henan Province (25A180017), and the Puyang Field Scientific Observation and Research Station for Yellow River Wetland Ecosystem, Henan Province.

References

Baguñà J, Carranza S, Pala M, Ribera C, Giribet G, Arnedo M, Ribas M, Riutort M (1999) From morphology and karyology to molecules. New methods for taxonomical identification of asexual populations of freshwater planarians. The Italian Journal of Zoology 66(3): 207–214. https://doi.org/10.1080/11250009909356258

Carranza S, Giribet G, Ribera C, Riutort M (1996) Evidence that two types of *18S* rDNA coexist in the genome of *Dugesia* (*Schmidtea*) *mediterranea* (Platyhelminthes, Turbellaria, Tricladida). Molecular Biology and Evolution 13(6): 824–832. https://doi.org/10.1093/oxfordjournals.molbev.a025643

Chen G-W, Wang L, Wu F, Sun X-J, Dong Z-M, Sluys R, Yu F, Yu-wen Y-Q, Liu D-Z (2022) Two new species of *Dugesia* (Platyhelminthes, Tricladida, Dugesiidae) from the subtropical monsoon region in Southern China, with a discussion on reproductive modalities. BMC Zoology 7(1): 25. https://doi.org/10.1186/s40850-022-00127-8

Cheng X-J, Fritsch P-W, Lin Y-J, Li G-H, Chen Y-Q, Zhang M-Y, Lu L (2024) The role of Pleistocene dispersal in shaping species richness of sky island wintergreens from the Himalaya-Hengduan Mountains. Molecular Phylogenetics and Evolution 197: 108082. https://doi.org/10.1016/j.ympev.2024.108082

Dessimoz C, Gil M (2010) Phylogenetic assessment of alignments reveals neglected tree signal in gaps. Genome Biology 11(4): R37. https://doi.org/10.1186/gb-2010-11-4-r37

Dong Z-M, Chen G-W, Zhang H-C, Liu D-Z (2017) A new species of *Polycelis* (Platyhelminthes, Tricladida, Planariidae) from China. Acta Zoologica Academiae Scientiarum Hungaricae 63(3): 263–276. https://doi.org/10.17109/AZH.63.3.263.2017

Dong F, Hung C-M, Yang X-J (2020) Secondary contact after allopatric divergence explains avian speciation and high species diversity in the Himalayan-Hengduan Mountains. Molecular Phylogenetics and Evolution 143: 106671. https://doi.org/10.1016/j.ympev.2019.106671

Favre A, Päckert M, Pauls S-U, Jähnig S-C, Uhl D, Michalak I, Muellner-Riehl A-N (2014) The role of the uplift of the Qinghai-Tibetan Plateau for the evolution of Tibetan biotas. Biological Reviews of the Cambridge Philosophical Society 90(1): 236–253. https://doi.org/10.1111/brv.12107

Harrath A-H, Mansour L, Sluys R, Aldahmich W, Alwasel S, Riutort M (2025) The first *Dugesia* species (Platyhelminthes, Tricladida, Dugesiidae) from Saudi Arabia: An integrative description. Zootaxa 5583(1): 113–127. https://doi.org/10.11646/zootaxa.5583.1.6

Ichikawa A, Kawakatsu M (1964) A new freshwater planarian, *Dugesia japonica*, commonly but erroneously known as *Dugesia gonocephala* (Dugès). Annotationes Zoologicae Japonenses 37: 185–194.

Kandziora M, Gehrke B, Popp M, Gizaw A, Brochmann C, Pirie M-D (2022) The enigmatic tropical alpine flora on the African sky islands is young, disturbed, and unsaturated. Proceedings of the National Academy of Sciences of the United States of America 119(22): e2112737119. https://doi.org/10.1073/pnas.2112737119

Katoh K, Rozewicki J, Yamada K-D (2019) MAFFT online service: Multiple sequence alignment, interactive sequence choice and visualization. Briefings in Bioinformatics 20(4): 1160–1166. https://doi.org/10.1093/bib/bbx108

Kawakatsu M, Mitchell R-W (1989) *Dugesia deharvengi* sp.nov., a new troglobitic freshwater planarian from Tham Kubio Cave, Thailand (Turbellaria; Tricladida; Paludicola). Nihon Seibutsu Chiri Gakkai Kaiho 44: 175–182.

Kawakatsu M, Oki I, Tamura S, Yamayoshi T (1985) Reexamination of freshwater planarians found in tanks of tropical fishes in Japan, with a description of a new species, *Dugesia austroasiatica* sp. nov. (Turbellaria; Tricladida; Paludicola). Nihon Seibutsu Chiri Gakkai Kaiho 40(1): 1–19.

Kawakatsu M, Takai M, Oki I, Tamura S, Aoyagi M. 1986. A note on an introduced species of freshwater planarian, *Dugesia austroasiatica* Kawakatsu, 1985, collected from culture ponds of *Tirapia mossambica* in Saga City, Kyûshû, Japan (Turbellaria, Tricladida, Paludicola). Bulletin of the Fuji Women's College no. 24, ser. II: 87–94.

Kumar S, Stecher G, Tamura K (2016) Mega7: Molecular evolutionary genetics analysis version 7.0 for bigger datasets. Molecular Biology and Evolution 33(7): 1870–1874. https://doi.org/10.1093/molbev/msw054

Lanfear R, Frandsen P-B, Wright A-M, Senfeld T, Calcott B (2017) PartitionFinder 2: New Methods for Selecting Partitioned Models of Evolution for Molecular and Morphological Phylogenetic Analyses. Molecular Biology and Evolution 34(3): 772–773. https://doi.org/10.1093/molbev/msw260

Lázaro E-M, Sluys R, Pala M, Stocchino G-A, Baguñà J, Riutort M (2009) Molecular barcoding and phylogeography of sexual and asexual freshwater planarians of the genus in the Western Mediterranean (Platyhelminthes, Tricladida, Dugesiidae). Molecular Phylogenetics and Evolution 52(3): 835–845. https://doi.org/10.1016/j.ympev.2009.04.022

Liu DZ. 1989. Freshwater planarians (Tricladida) of China. Chinese Journal of Zoology 24(6): 38–43, 31. [in Chinese]

Liu R, Wang H, Yang J-B, Corlett R-T, Randle C-P, Li D-Z, Yu W-B (2022a) Cryptic species diversification of the *Pedicularis siphonantha* complex (Orobanchaceae) in the Mountains of Southwest China since the Pliocene. Frontiers in Plant Science 13: 811206. https://doi.org/10.3389/fpls.2022.811206

Liu Y, Song X-Y, Sun Z-Y, Li W-X, Sluys R, Li S-F, Wang A-T (2022b) Addition to the known diversity of Chinese freshwater planarians: Integrative description of a new species of *Dugesia* Girard, 1850 (Platyhelminthes, Tricladida, Dugesiidae). Zoosystematics and Evolution 98(2): 233–243. https://doi.org/10.3897/zse.98.83184

Liu R, Wang W-J, Wang H, Ree R-H, Li D-Z, Yu W-B (2024) Plant species diversification in the Hinalya-Hengduan Mountains region: An example from an endemic lineage of *Pedicularis* (Orobanchaceae) in the role of floral specializations and rapid range expansions. Cladistics 40(6): 636–652. https://doi.org/10.1111/cla.12596

Nguyen L-T, Schmidt H-A, Haeseler A, Minh B-Q (2015) IQ-TREE: A Fast and Effective Stochastic Algorithm for Estimating Maximum-Likelihood Phylogenies. Molecular Biology and Evolution 32(1): 268–274. https://doi.org/10.1093/molbev/msu300

Qu Y-H, Ericson P-G-P, Lei F, Gebauer A, Kaiser M, Helbig A-J (2006) Molecular phylogenetic relationship of snow finch complex (genera *Montifringilla*, *Pyrgilauda*, and *Onychostruthus*) from the Tibetan plateau. Molecular Phylogenetics and Evolution 40(1): 218–226. https://doi.org/10.1016/j.ympev.2006.02.020

Rambaut A, Drummond A-J, Xie D, Baele G, Suchard M-A (2018) Posterior Summarization in Bayesian Phylogenetics Using Tracer 1.7. Systematic Biology 67(5): 901–904. https://doi.org/10.1093/sysbio/syy032

Ronquist F, Teslenko M, Mark P, Ayres D-L, Darling A, Höhna S, Larget B, Liu L, Suchard M-A, Huelsenbeck J-P (2012) MrBayes 3.2: Efficient Bayesian Phylogenetic Inference and Model Choice Across a Large Model Space. Systematic Biology 61(3): 539–542. https://doi.org/10.1093/sysbio/sys029

Shi B-Y, Pan D, Zhang K-Q, Gu T-Y, Yeo D-C, Ng P-K, Sun H-Y (2023) Diversification of freshwater crabs on the sky islands in the Hengduan Mountains Region, China. Molecular Phylogenetics and Evolution 190: 107955. https://doi.org/10.1016/j.ympev.2023.107955

Sluys R, Kawakatsu M, Winsor L (1998) The genus *Dugesia* in Australia, with its phylogenetic analysis and historical biogeography (Platyhelminthes, Tricladida, Dugesiidae). Zoologica Scripta 27(4): 273–289. https://doi.org/10.1111/j.1463-6409.1998.tb00461.x

Solà E, Sluys R, Gritzalis K, Riutort M (2013) Fluvial basin history in the northeastern Mediterranean region underlies dispersal and speciation patterns in the genus (Platyhelminthes, Tricladida, Dugesiidae). Molecular Phylogenetics and Evolution 66(3): 877–888. https://doi.org/10.1016/j.ympev.2012.11.010

Solà E, Leria L, Stocchino G-A, Bagherzadeh R, Balke M, Daniels S-R, Harrath A-H, Khang T-F, Krailas D, Kumar B, Li M-H, Maghsoudlou A, Matsumoto M, Naser N, Oben B, Segev O, Thielicke M, Tong X, Zivanovic G, Manconi R, Baguñà J, Riutort M (2022) Three dispersal routes out of Africa: A puzzling biogeographical history in freshwater planarians. Journal of Biogeography 49(7): 1219–1233. https://doi.org/10.1111/jbi.14371

Stocchino G-A, Sluys R, Manconi R (2012) A new species of *Dugesia* (Platyhelminthes, Tricladida, Dugesiidae) from the Afromontane forest in South Africa, with an overview of freshwater planarians from the African continent. Zootaxa 3551(1): 43–58. https://doi.org/10.11646/zootaxa.3551.1.3

Stocchino G-A, Sluys R, Riutort M, Solà E, Manconi R (2017) Freshwater planarian diversity (Platyhelminthes: Tricladida: Dugesiidae) in Madagascar: new species, cryptic species, with a redefinition of character states. Zoological Journal of the Linnean Society 181(4): 727–756. https://doi.org/10.1093/zoolinnean/zlx017

Stocchino G-A, Sluys R, Solà E, Riutort M, Manconi R (2024) The long-eared freshwater planarians of Madagascar form a separate phylogenetic clade within the genus *Dugesia* (Platyhelminthes: Tricladida), with the description of two new species. Zoological Journal of the Linnean Society 202(4): zlae143. https://doi.org/10.1093/zoolinnean/zlae143

Tamura K, Stecher G, Peterson D, Filipski A, Kumar S (2013) MEGA6: Molecular Evolutionary Genetics Analysis Version 6.0. Molecular Biology and Evolution 30(12): 2725–2729. https://doi.org/10.1093/molbev/mst197

Wang L, Chen J-Z, Dong Z-M, Chen G-W, Sluys R, Liu D-Z (2021) Two new species of *Dugesia* (Platyhelminthes, Tricladida, Dugesiidae) from the tropical monsoon forest in Southern China. ZooKeys 1059: 89–116. https://doi.org/10.3897/zookeys.1059.65633

Wang L, Wang Y, Dong Z, Chen G, Sluys R, Liu D (2022) Integrative taxonomy unveils a new species of *Dugesia* (Platyhelminthes, Tricladida, Dugesiidae) from the southern portion of the Taihang Mountains in northern China, with the description of its complete mitogenome and an exploratory analysis of mitochondrial gene order as a taxonomic character. Integrative Zoology 17(6): 1193–1214. https://doi.org/10.1111/1749-4877.12605

Wang L, Zhu S-Q, Ma F-H, Li X-J, Zhao Y-H, Sun X-X, Li N, Sluys R, Liu D-Z, Dong Z-M, Chen G-W (2024) Two new species of freshwater planarian (Platyhelminthes, Tricladida, Dugesiidae, *Dugesia*) from Southern China exhibit unusual karyotypes, with a discussion on reproduction in aneuploid species. Journal of Zoological

Systematics and Evolutionary Research 2024: 1–18. https://doi.org/10.1155/2024/8299436

Wang L, Chang Y-F, Sun X-X, Sluys R, Liu D-Z, Dong Z-M, Chen G-W (2025) Two new species of *Dugesia* from Hainan Island and Leizhou Peninsula (Platyhelminthes, Tricladida, Dugesiidae). ZooKeys 1233: 289–313. https://doi.org/10.3897/zookeys.1233.142976

Winsor L, Sluys R 2018. Basic histological techniques for planarians. In: Rink JC (Ed.) Planarian Regeneration: Methods and Protocols, Methods in Molecular Biology, vol. 1774, Humana Press, Springer Science+Business Media, 285–351. https://doi.org/10.1007/978-1-4939-7802-1_9

Xing Y-W, Ree R-H (2017) Uplift-driven diversification in the Hengduan Mountains, a temperate biodiversity hotspot. Proceedings of the National Academy of Sciences of the United States of America 114(17): E3444–E3451. https://doi.org/10.1073/pnas.1616063114

Zhu Y, Huang J, Sluys R, Liu Y, Sun T, Wang A-T, Zhang Y (2024) Integrative description of a new species of *Dugesia* (Platyhelminthes, Tricladida, Dugesiidae) from Southern China, with its complete mitogenome and a biogeographic evaluation. Zoosystematics and Evolution 100(1): 167–182. https://doi.org/10.3897/zse.100.114016

Supplementary material 1

Additional figures

Authors: Fan Wu, Lei Wang, Ronald Sluys, Xin-Xin Sun, De-Zeng Liu, Zi-Mei Dong, Guang-Wen Chen1

Data type: pdf

Explanation note: **fig. S1.** Phylogenetic tree obtained from ML analysis of the concatenated dataset. Numbers at nodes indicate support values (bootstrap). New species indicated in red. **fig. S2.** Phylogenetic tree obtained from ML analysis of the COI gene dataset. Numbers at nodes indicate support values (bootstrap). New species indicated in red. **fig. S3.** Phylogenetic tree obtained from ML analysis of the ITS-1 gene dataset. Numbers at nodes indicate support values (bootstrap). New species indicated in red. **fig. S4.** Phylogenetic tree obtained from ML analysis of the 28S gene dataset. Numbers at nodes indicate support values (bootstrap). New species indicated in red. **fig. S5.** Phylogenetic tree obtained from ML analysis of the 18S gene dataset. Numbers at nodes indicate support values (bootstrap). New species indicated in red.

Link: https://doi.org/10.3897/zse.101.156742.suppl1

Supplementary material 2

Genetic distances for COI

Authors: Fan Wu, Lei Wang, Ronald Sluys, Xin-Xin Sun, De-Zeng Liu, Zi-Mei Dong, Guang-Wen Chen1

Data type: xls

Explanation note: The highest and lowest distance values between the two new species and congeners are indicated in blue and red, respectively.

Link: https://doi.org/10.3897/zse.101.156742.suppl2

Supplementary material 3

Genetic distances for ITS-1

Authors: Fan Wu, Lei Wang, Ronald Sluys, Xin-Xin Sun, De-Zeng Liu, Zi-Mei Dong, Guang-Wen Chen1

Data type: xls

Explanation note: The highest and lowest distance values between the two new species and congeners are indicated in blue and red, respectively.

Link: https://doi.org/10.3897/zse.101.156742.suppl3